EPJ Web of Conferences **271**, 01004 (2022) https://doi.org/10.1051/epjconf/202227101004
HYP2022

Single- & double-strangeness hypernuclei up to A = 8 within χEFT

Hoai Le[1,*]

[1]IAS-4, IKP-3 and JHCP, Forschungszentrum Jülich, D-52428 Jülich, Germany

Abstract. We investigate S=-1 and -2 hypernuclei with A = 4 – 8 employing the Jacobi-NCSM approach and in combination with baryon-baryon interactions derived within the frame work of chiral effective field theory. The employed interactions are transformed using the similarity renormalization group (SRG) so that the low- and high-momentum states are decoupled, and, thereby, convergence of the binding energies with respect to model space can be significantly speeded up. Such an evolution is however only approximately unitary when the so-called SRG induced higher-body forces are omitted. We first explore the impact of the SRG evolution on the Λ separation energies B_Λ in A = 3 – 5 hypernuclei when only SRG-evolved two-body and when both two- and three-body forces are included. For the latter scenario, we thoroughly study predictions of the two almost phase-equivalent NLO13 and NLO19 YN potentials for A = 4 – 7 hypernuclei. We further explore CSB splittings in the A = 7, 8 multiplets employing the two NLO YN potentials that include also the leading CSB potential in the ΛN channel, whose strength has been fitted to the presently established CSB in A = 4. Finally, we report on our recent study for Ξ hypernuclei based on the ΞN interaction at NLO.

1 Introduction

Experimental information on hyperon-nucleon (YN) and hyperon-hyperon (YY) scattering data is indispensable input for developing realistic YN and YY interactions [1–6]. However, despite significant progress over the last several decades, scattering data in the strangeness S=-1,-2 sectors remain extremely scarce and the situation is not expected to be substantially improved in the near future. Yet, other important source of information is hypernucler spectroscopy [7], in which not only ground-state energies but also energy level splittings in single- and double-strangness systems can be determined with high accuracy. This together with theoretical studies of hypernuclei, especially with microscopic approaches are essential tools to explore the underlying baryon-baryon (BB) interactions and thereby to improve interactions models.

In this study, we investigate single-Λ and Ξ hypernuclear systems with A=4 - 8 based on the "ab initio" Jacobi no-core shell model (NCSM) [8, 9] and in combination with BB interactions derived within chiral effective field theory (EFT). In this approach, potentials are established in terms of an expansion in powers of low momenta in accordance with an appropriate power counting scheme. The long-ranged parts of the interactions are fixed from chiral symmetry, whereas unresolved short-distance dynamics are parameterized in terms of

*e-mail: h.le@fz-juelich.de

© The Authors, published by EDP Sciences. This is an open access article distributed under the terms of the Creative Commons Attribution License 4.0 (http://creativecommons.org/licenses/by/4.0/).

the so-called low energy constants (LECs), whose strengths should be determined via a fit to experiments. In the non-strangeness sector, thanks to the wealth of NN scattering data, two- and three-body interactions have been consistently derived up to high order, e.g. N^{4}LO [10] and N^{2}LO [11], respectively, see also Ref. [12] for an overview on the current status of the chiral NN and 3N interactions. In the S=-1,-2 sectors, the situation is however less satisfactory due to, as already said, the lack of the appropriate scattering data. Despite of that, YN and YY potentials up to NLO have been derived [2–5] and recently extended to N^{2}LO [6]. Especially, at NLO, by pursuing different strategies for fixing LECs, two realizations of the YN interaction, NLO13 [2] and NLO19 [3], which yield similarly good description of all the available YN scattering data, could be established. However, as discussed in [3], NLO19 is characterized by a somewhat weaker ΛN – ΣN transition potential, and as a result, the two potentials yield slightly different predictions for ${}^{4}_{\Lambda}$He and for nuclear matter. Also, in [9] we have explored effects of NLO13 and NLO19 on light hypernuclei with A=4 - 7, but only qualitatively. Below we revisit this topic and take a closer look at the separation energies of these systems predicted by the two potentials, and thereby, discuss the possible effect of chiral YNN forces. In addition, we explore charge symmetry breaking (CSB) effects in the A=7, 8 multiplets, employing the NLO13 and NLO19 interactions and with the inclusion of the leading CSB potential derived in Ref. [16]. The latter involves additional two LECs that have been determined via a fit to the separation energies difference ΔB_Λ in the ground and excited states of ${}^{4}_{\Lambda}$He and ${}^{4}_{\Lambda}$H, with $\Delta B_\Lambda(0^+) = 233 \pm 92$ keV and $\Delta B_\Lambda(1^+) = -83 \pm 94$ [17], respectively. Finally, we discuss our recent work [13], where the possible existence of Ξ hypernuclei up to A=7 for the NLO ΞN potential [5] has been explored.

2 SRG evolution for YN NLO and impact on B_Λ in A=3-5 hypernuclei

BB interactions generally contain short-range and tensor correlations that couple low- and high-momentum states, which make calculations expanded in harmonic oscillator (HO) bases such as the NCSM converge slowly. A very large number of HO functions is required in order to incorporate such strong correlations and therefore well-converged results for systems with $A \geq 5$ are practically computationally inaccessible. So, in order soften the interactions we will continuously evolve the Hamiltonian using the Similarity Renormalization Group (SRG). The latter can be written in term of a flow equation for potentials, which, in three-body YNN space, has following form

$$\frac{dV_s}{ds} = [[T_{\rm rel}, V_s], H_s]; \quad H_s = T_{\rm rel} + V_s + \Delta{\rm M} = T_{\rm rel} + V^{\rm NN}_{12,s} + V^{\rm YN}_{32,s} + V^{\rm YN}_{31,s} + V^{\rm YNN}_{s} + \Delta{\rm M}. \quad (1)$$

Here $T_{\rm rel}$ is the intrinsic kinetic energy, ΔM is the rest mass difference arising due to particle conversions such as ΛN – ΣN, and s is a flow parameter that varies from 0 to ∞ with $s = 0$ meaning no evolution or bare interactions. For characterising SRG-evolved interactions, we will however use the more intuitive λ parameter, $\lambda = (4\mu_{\rm N}^2/s)^{1/4}$ with $\mu_{\rm N}$ being nucleon reduced mass, that provides a measure of the width of the potentials in momentum space [18]. We solve the flow equation Eq. (1) in momentum space and follow the same approach as done in [18, 19] that explicitly separates the flow equations for two-body NN and YN, and three-body YNN interactions by employing the relation $\frac{dV_s}{ds} = \frac{dV^{\rm NN}_{12,s}}{ds} + \frac{dV^{\rm YN}_{32,s}}{ds} + \frac{dV^{\rm YN}_{31,s}}{ds} + \frac{dV^{\rm YNN}_{s}}{ds}$. In two-body NN and YN space, the flow equations for $V^{\rm NN}$ and $V^{\rm YN}$ can be written as [9]

$$\frac{dV^{\rm NN}_{12}}{ds} = [[t^{\rm NN}_{12}, V^{\rm NN}_{12}], t^{\rm NN}_{12} + V^{\rm NN}_{12}]$$
$$\frac{dV^{\rm YN}_{32}}{ds} = [[t^{\rm YN}_{32}, V^{\rm YN}_{32}], t^{\rm YN}_{32} + V^{\rm YN}_{32} + \Delta{\rm M}]; \qquad \frac{dV^{\rm YN}_{31}}{ds} = [[t^{\rm YN}_{31}, V^{\rm YN}_{31}], t^{\rm YN}_{31} + V^{\rm YN}_{31} + \Delta{\rm M}], \quad (2)$$

hence, the evolution equation for $V^{\rm YNN}$ reads,

$$\frac{dV^{\rm YNN}}{ds} = [[t_{12}^{\rm NN}, V_{12}^{\rm NN}],\, V_{32}^{\rm YN} + V_{31}^{\rm YN} + V^{\rm YNN}] + [[t_{32}^{\rm YN},\, V_{32}^{\rm YN}], V_{12}^{\rm NN} + V_{31}^{\rm YN} + V^{\rm YNN}] \quad (3)$$
$$+[[t_{31}^{\rm YN}, V_{31}^{\rm YN}], V_{32}^{\rm YN} + V_{12}^{\rm NN} + V^{\rm YNN}] + [[T_{\rm rel}, V^{\rm YNN}], T_{\rm rel} + V_{12}^{\rm NN} + V_{32}^{\rm YN} + V_{31}^{\rm YN} + V^{\rm YNN} + \Delta{\rm M}]$$

Note that now the Kronecker delta functions that appear when embedding two-body interactions in a three-body YNN basis, see the right hand side of Eq. (3), can be evaluated analytically [18, 19]. By projecting Eqs.(2,3) onto the corresponding two- and three-body partial-decomposed momentum-space bases, we obtain a system of coupled ordinary differential equations which will be solved simultaneously employing the ARKsover from SUNDIAL. In the current work, we do not include chiral YNN forces in the evolution, however, it should be clear from Eq. (3) that the SRG evolution will eventually induce three-body YNN interactions even if the initial (bare) potential $V_{s=0}^{\rm YNN}$ is set to zero. Therefore, omitting those induced higher-body forces, the SRG evolution will only be approximately unitary. Indeed, as it can clearly be seen in Fig. 1, the binding energies (square blue symbols) of the A = 3 − 5 hypernuclei, computed for SRG-evolved NN and YN interactions, exhibit a strong dependence on the λ flow parameter. With the inclusion of the induced YNN forces, we practically reproduce the hypertrition binding energy $E(^3_\Lambda{\rm H})$ (dashed green line) that was obtained when solving the Faddeev equation for the bare NN and YN potentials, see panel (a) in Fig. 1. Note the large estimated errors for the NCSM results because of the extremely small separation energy of $^3_\Lambda$H. In panel (b), we clearly demonstrate that $E(^3_\Lambda{\rm H})$ is indeed independent of the SRG parameter by increasing the strength of the YN interaction, say, by a factor of 1.5, so that the $^3_\Lambda$H hypernucleus is more tightly bound. Similarly, with both SRG-induced YNN and 3N forces included, the SRG-dependence of B_Λ in the A = 4, 5 systems is significantly removed, as clearly shown in panels (c-d). This is an important indication of likely negligibly small contributions of SRG-induced higher-body forces to the separation energies of these systems. However, for a more quantitative estimate of those contributions, well-converged separation energies computed for a wide range of flow parameter are required.

3 Effect of NLO YN interactions on B_Λ in A = 4 − 7 hypernuclei

In our work [9], using only SRG-evolved NN and YN forces, we have qualitatively studied predictions of the two practically phase equivalent NLO13 and NLO19 YN interactions for the separation energies in the A = 4 − 7 systems. Overall, the NLO19 potential, that is characterized by a weaker ΛN − ΣN transition potential [3], yields substantially larger B_Λ in all systems considered except for $^4_\Lambda$H/$^4_\Lambda$He(0^+), see Fig. 10 in Ref.[9]. As also discussed in that work, such a large discrepancy between the NLO13 and NLO19 predictions could be attributed to possible contributions of chiral YNN forces, which according to the underlying power counting will appear at N^{2}LO [6, 20]. Now, taking into account both chiral and SRG-induced 3N interactions as well as SRG-induced YNN forces, we can study the actual separation energies predicted by the two YN potentials in more detail. These results together with the experimental B_Λ for the A = 4 − 7 hypernuclei are summarized in Table. 1. One sees that NLO13 and NLO19 yield very similar separation energies for the $^4_\Lambda$H(0^+) state, with B_Λ = 1.551 ± 0.007 MeV and 1.514 ± 0.007 MeV, respectively, that are by roughly 0.6 MeV smaller than the empirical value of B_Λ = 2.16 ± 0.08 MeV [21]. Likewise, the separation energies for $^4_\Lambda$H(1^+) and the ground states in $^5_\Lambda$He and $^7_\Lambda$Li computed for NLO13 are 0.823 ± 0.003 MeV, 2.22 ± 0.06 MeV and 5.28 ± 0.68, respectively. In comparison with the empirical B_Λ of 1.07 ± 0.08 MeV, 3.12 ± 0.02 MeV and 5.58 ± 0.03 MeV [21], respectively, the NLO13 potential clearly underestimates these systems. In contrast, the predictions

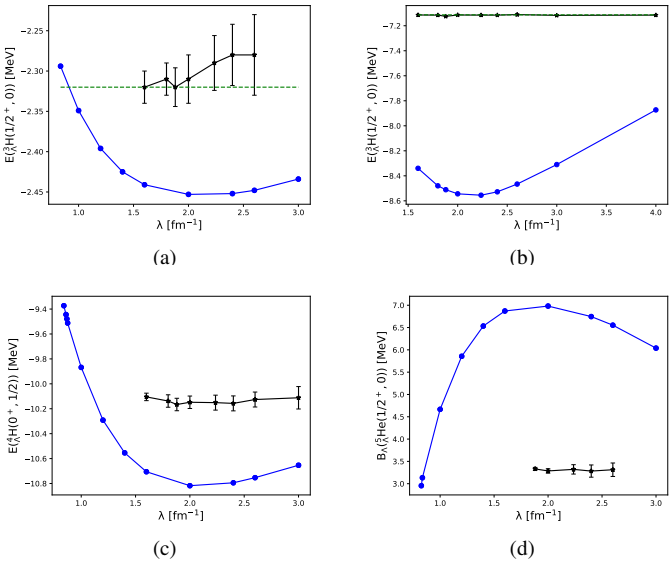

Figure 1. Dependence of the binding (separation) energies in A = 3 − 5 hypernuclei on λ flow parameter. The results (blue circles, panels (a, c,d)) are computed using the SMS N^{4}LO$^+$450 [10] NN potential SRG-evolved to λ_{NN} = 1.6 fm^{-1} and the NLO13(500) YN interaction (with CSB included) evolved to a wide range of flow parameter. In panel (b) the strength of the original NLO13 potential is amplified by a factor of 1.5 so that ${}^{3}_{\Lambda}$H is more tightly bound. Black triangles are obtained with inclusion of SRG-induced YNN (panels (a-b)) and of the 3N forces [11] (panels (c-d)). Dashed green lines are binding energies computed by solving the Faddeev equation for the bare NN and YN interactions.

	${}^{4}_{\Lambda}$H		${}^{5}_{\Lambda}$He	${}^{7}_{\Lambda}$Li
	0^+	1^+	$1/2^+$	$(1/2^+, 0)$
NLO13(500)	1.551 ± 0.007	0.823 ± 0.003	2.22 ± 0.06	5.28 ± 0.68
NLO19(500)	1.514 ± 0.007	1.27 ± 0.009	3.32 ± 0.03	6.04 ± 0.30
Exp [21, 22]	2.16 ± 0.08	1.07 ± 0.08	3.12 ± 0.02	5.85 ± 0.13(10) 5.58 ± 0.03

Table 1: B_Λ for the A = 4 − 7 hypernuclei computed for the YN potentials NLO13(500) and NLO19(500) including the CSB interaction. The SMS N^{4}LO$^+$(450) and N^{2}LO(450) are used to describe the 2N and 3N interactions, respectively. All the employed potentials are evolved to a SRG parameter of λ = 1.88 fm^{-1}. SRG-induced YNN forces are explicitly taken into account. All energies are given in MeV.

of NLO19 for these three states are quite close to experiment, only slightly above. For example, the computed separation energies for ${}^{4}_{\Lambda}$H(1^+) and ${}^{5}_{\Lambda}$He, $B_\Lambda({}^{4}_{\Lambda}\mathrm{H}, 1^+)) = 1.27 \pm 0.009$ and $B_\Lambda({}^{5}_{\Lambda}\mathrm{He}) = 3.32 \pm 0.03$, exceed the experiment by less than 0.2 MeV. Interestingly, for the ground state of ${}^{7}_{\Lambda}$Li we obtained the value of $B_\Lambda = 6.04 \pm 0.30$ MeV, that is somewhat larger than the emulsion separation energy, $B_\Lambda = 5.58 \pm 0.03$ [21], but it is in perfect agreement with the one deduced from counter experiments, with $B_\Lambda = 5.85 \pm 0.13(10)$ [22]. In conclusion, the discrepancies between B_Λ predicted by NLO13 and NLO19, and between the computed B_Λ and experiment could be an indication of the importance of YNN forces for properly describing light hypernuclei within the χ EFT approach.

4 CSB in $A = 7, 8$ isospin multiplets

Being able to accurately compute hypernuclear wave functions for hypernuclei up to the *p*-shell, we can now employ those wave functions to explore CSB effects in the A = 7, 8 multiplets. Here, we employ the NLO13(500) and NLO19(500) potentials both without and with CSB components [16] as YN interactions, while the SMS N^{4}LO$^+$(450) [10] and N^{2}LO(450)

		ΔT	ΔV_{NN}	ΔV_{YN}			ΔB_Λ
				$^1S_0$	$^3S_1$	total	
$^7_\Lambda$Be-$^7_\Lambda$Li*	NLO13	7	-24	-1	0	0	-17
	NLO13-CSB	8	-24	-49	26	-24	-40
	NLO19	6	-40	-1	0	0	-34
	NLO19-CSB	6	-41	-43	42	9	-35
	Hiyama [25]		-70			200	150
	Gal [24]	3	-70			50	-17
	experiment [17]						-100 ± 90
$^8_\Lambda$Be-$^8_\Lambda$Li	NLO13	12	8	-2	0	-4	16
	NLO13-CSB	12	7	100	56	159	178
	NLO19	7	-11	-1	0	-2	-6
	NLO19-CSB	6	-11	62	79	147	143
	Hiyama [25]		40				160
	Gal [24]	11	-81			119	49
	experiment [26]						40 ± 60

Table 2: Contributions to CSB in the A = 7 and 8 isospin multiplets, based on the YN potentials NLO13(500) and NLO19(500) (including 3N and SRG-induced YNN forces). The results are for the original potentials (i.e. without CSB force) and for the scenario CSB1 [16]. The estimated uncertainties for ΔB_Λ in A = 7, 8 multiplets are 30 and 50 keV, respectively (see the text). All energies are in keV.

[11] are used for NN and 3N interactions, respectively. All the employed potentials are evolved to a SRG parameter of $\lambda = 1.88$ fm^{-1}. In addition, both YNN and 3N forces that are generated during the evolution are explicitly included in all calculations. Let us further remark that, as one can also see in Table. 1, due to the limited accessible model space, B_Λ for systems with A $\geq$ 7 are afflicted with rather large uncertainties, which even exceed the experimentally found CSB splittings in those systems. Therefore, it will be more meaningful to extract the CSB results for the A = 7, 8 multiplets perturbatively based on the $^7_\Lambda$Li*(T = 1) and $^8_\Lambda$Li(T = 1/2) hypernuclear wave functions and the ^{6}Li*(T = 1) and ^{7}Li(T = 1/2) nuclear wave functions, respectively. Note that this perturbative treatment has been also applied to study CSB effects in the A = 4 systems in Ref. [16]. The employed wave functions are computed for the largest computationally accessible model space, namely $\mathcal{N}_{\max} = 10\,(9)$ for A = 7 (8), and for the optimal HO frequency $\omega_{\rm opt} = 16$ MeV that yields the lowest binding energies. For estimating the uncertainty, we will consider only two-body interactions and perform calculations using the model space $\mathcal{N} = \mathcal{N}_{\max}$, $\mathcal{N}_{\max} + 2$, and at the HO frequencies $\omega = \omega_{\rm opt} \pm 2$ MeV. The variation of the CSB results compared to the values obtained at $\mathcal{N}_{\max}$ and $\omega_{\rm opt}$ will be assigned as the uncertainty of our CSB estimations which amount to 30 (50) keV for A = 7 (8). Note that the latter is of the same magnitude as that for the uncertainties of the CSB results deduced from experiment, therefore, a direct comparison of our CSB predictions with experiment is possible.

Details of the computed CSB splittings for the mirror hypernuclei ($^7_\Lambda$Be-$^7_\Lambda$Li*) and ($^8_\Lambda$Be-$^8_\Lambda$Li) are summarized in Table. 2, where individual contributions of the kinetic energy ΔT, of the NN interaction $\Delta V_{\rm NN}$ and of the YN potential $\Delta V_{\rm YN}$ to the total CSB are also provided. Note that the 3N and SRG-induced YNN forces contributions are insignificantly small, they are therefore omitted from the table. Furthermore, in order to understand the relation between the CSB effect of the employed YN potentials and the $\Delta V_{\rm YN}$ for larger systems, which as shown in [16] contributes dominantly to the CSB splitting in the A = 4 doublets, we also estimate the $^1S_0$ and $^3S_1$ partial-wave contributions to $\Delta V_{\rm YN}$ separately.

One clearly sees that, despite the substantial discrepancies in their predicted B_Λ, the two YN potentials yield comparable CSB results in the A = 7 mutiplets. For both cases, with and without the CSB interactions included, the overall CSB effects are small and consistent with the experiment both in magnitude and in sign. It is further observed that the $^1S_0$ and $^3S_1$ states contribute with opposite signs to the total $\Delta V_{\rm YN}$, like that for the 1^+ states in the A = 4 systems [23], which in turns leads to a small total CSB in the A = 7 isotriplet. Surprisingly, our prediction for $^7_\Lambda$Be-$^7_\Lambda$Li* for the original NLO13 potential (i.e. without CSB components), with ΔB_Λ(NLO13) = -17 keV, is identical to the value estimated by Gal [24], for which a simple shell-model approach in combination with effective potentials were employed. However, the individual contributions ΔT, $\Delta V_{\rm NN}$, and $\Delta V_{\rm YN}$ differ substantially. For example,

the original NLO13 yields a vanishing $\Delta V_{\rm YN}$, whereas in Gal's calculation this contribution amounts to 50 keV. That value is also of opposite sign and larger than our estimated $\Delta V_{\rm YN}$ for the actual CSB potential. In addition, our NCSM estimate for $\Delta V_{\rm NN}$ (that also includes the Coulomb effect) is visibly smaller than the corresponding one used in Gal's calculation. Note that the latter is not computed consistently but rather taken from a cluster-model study of Hiyama *et al.* [25].

CSB results for ${}^{8}_{\Lambda}$Be-${}^{8}_{\Lambda}$Li are listed at the lower end of Table 2. Without the CSB components, the two NLO13 and NLO19 potentials predict a negligibly small CSB for ${}^{8}_{\Lambda}$Be-${}^{8}_{\Lambda}$Li, with $\Delta B_\Lambda = 16 \pm 50$ keV and -6 ± 50 keV, respectively, which are well in line with the separation energies difference of 40 ± 60 keV [26] deduced from emulsion data. A similarly small ΔB_Λ was also predicted by Gal in [24]. However, in contrast to the rather small $\Delta V_{\rm NN}$ contribution in our calculation, e.g. $\Delta V_{\rm NN} = -11$ keV for NLO19, Gal assigned a significantly larger value to $\Delta V_{\rm NN}$, with $\Delta V_{\rm NN} = -81$ keV that was taken from a shell model calculation by Millener [24]. Clearly, the individual contributions to ΔB_Λ are rather model-dependent, hence, it is very important that they are computed consistently. Interestingly, with the CSB potentials included, both NLO13 and NLO19 yield rather sizable CSB results, $\Delta B_\Lambda = 177 \pm 50$ keV and 143 ± 50 keV, respectively. In this case, the ${}^1S_0$ and ${}^3S_1$ partial-wave contributions are also large, and importantly, of the same sign, adding up to a pronounced total CSB. We found that this exactly resembles the situation for the 0^+ states of the A = 4 mirror hypernuclei [23]. One could therefore conclude that a fairly large splitting in the A = 4(0^+) states, as presently suggested by experiments [17], implies automatically a likewise significant CSB splitting in ${}^{8}_{\Lambda}$Be–${}^{8}_{\Lambda}$Li. Interestingly, the predictions of NLO13 and NLO19 with CSB interaction are comparable to the value of $\Delta B_\Lambda = 160$ keV obtained in a three-body cluster calculation by Hiyama *et al.* [25]. However, it should be stressed that the phenomenological CSB YN interaction employed in that work was fitted to an outdated CSB splittings for the A = 4 doublets, namely $\Delta B_\Lambda(0^+) = 350 \pm 60$ keV and $\Delta B_\Lambda(1^+) = 240 \pm 60$ keV. Also it was estimated there that the Coulomb interaction contributes about -80 keV to ΔB_Λ, which is substantially larger than our estimate of roughly 10 keV.

5 Results for A = 4 − 7 Ξ hypernuclei

In this section we discuss the results for A = 4 − 7 Ξ hypernuclei based on our recent study in Ref. [13]. Here all the calculations have been computed using the SMS N^{4}LO$^+$(450) NN [10] and NLO(500) ΞN [5] interactions. The original ΞN potential includes coupling to all other baryon-baryon channels in the $S = -2$ sector such as ΛΛ, ΛΣ and ΣΣ. However, in practice, the coupling ΛΛ − ΞN was omitted here and its contribution is effectively incorporated by appropriately re-adjusting the strength of the $V_{\Xi{\rm N}-\Xi{\rm N}}$ potential [13]. This facilitates a proper convergence of the energy calculations to the lowest lying Ξ state. Furthermore, the employed NN and ΞN potentials are evolved to a SRG flow parameter of $\lambda_{\rm NN} = \lambda_{\Xi{\rm N}} = 1.6$ fm^{-1}. For simplicity, the electromagnetic NN interaction [27] as well as the Coulomb point-like interaction between Ξ^- and a proton are only included after the evolution. And, SRG-induced higher-body forces are not included in that study. As a result, we observe a moderate dependence of the Ξ separation energies B_Ξ on the $\lambda_{\Xi{\rm N}}$ parameter [13]. However, the overall SRG dependence of B_Ξ is relatively small as compared to the actual separation energies, and therefore, it should not affect our conclusion on the existence of the found bound state [13].

The computed separation energies B_Ξ of A = 4 − 7 Ξ hypernuclei together with their perturbatively estimated decay width Γ are provided in Table 3 . It is estimated that the $\Xi^- p$ Coulomb interaction contributes only moderately to the total binding energies of the NNNΞ, ${}^{5}_{\Xi}$H and ${}^{7}_{\Xi}$H systems, about 0.2, 0.6, and 0.4 MeV, respectively. Thus, the binding of these systems should be predominantly due to the strong ΞN interaction. Overall, we

	B_Ξ [MeV]	Γ [MeV]
${}^{4}_{\Xi}\mathrm{H}(1^+, 0)$	0.48 ± 0.01	0.74
${}^{4}_{\Xi}\mathrm{n}(0^+, 1)$	0.71 ± 0.08	0.2
${}^{4}_{\Xi}\mathrm{n}(1^+, 1)$	0.64 ± 0.11	0.01
${}^{4}_{\Xi}\mathrm{H}(0^+, 0)$	-	-
${}^{5}_{\Xi}\mathrm{H}(\frac{1}{2}^+, \frac{1}{2})$	2.16 ± 0.10	0.19
${}^{7}_{\Xi}\mathrm{H}(\frac{1}{2}^+, \frac{3}{2})$	3.50 ± 0.39	0.2

Table 3: Ξ separation energies B_Ξ and estimated decay widths Γ for $A = 4 - 7$ Ξ hypernuclei. All calculations are based on the NLO(500) YY-ΞN interaction and the SMS N^{4}LO+(450) NN potential. Both interactions are SRG-evolved to a flow parameter of $\lambda_{\mathrm{NN}} = \lambda_{\Xi\mathrm{N}} = 1.6$ fm^{-1}. The values of B_Ξ in NNNΞ, ${}^{5}_{\Xi}$H and ${}^{7}_{\Xi}$H are measured with respect to the binding energies of the core nuclei ^{3}H, ^{4}He and ^{6}He, respectively.

found three weakly bound states $(1^+, 0)$, $(0^+, 1)$ and $(1^+, 1)$ in NNNΞ, with quite similar B_Ξ's but substantially different decay widths. Interestingly, our result for the NNN$\Xi(1^+, 0)$ state, $B_\Xi = 0.48 \pm 0.01$ MeV, is close to the value of 0.36 ± 0.16 MeV obtained with the HAL QCD potential [28]. The latter however does not support the binding of the two $(0^+, 1)$ and $(1^+, 1)$ states. In addition, there are substantial differences between our separation energies B_Ξ(NNNΞ) and the results for the ESC08c potential [29] also reported in [28]. Note that this version of the Nijmegen potential predicts an unrealistically large strength for the ΞN interaction in the ${}^{33}S_1$ state that even results in a bound ΞN state.

Our computed separation energy and decay width for ${}^{5}_{\Xi}$H are $B_\Xi = 2.16 \pm 0.1$ MeV and $\Gamma = 0.19$ MeV. Surprisingly, these values agree roughly with the estimations by Myint and Akaishi [30] of 1.7 MeV and 0.2 MeV, respectively. However, in contrast to our finding that ${}^{5}_{\Xi}$H is bound primarily due to the strong ΞN interaction, the authors in [30] estimated that most of the 1.7 MeV binding energy comes from the ^{4}He-Ξ^- Coulomb interaction. A quite similar separation energy, $B_\Xi({}^{5}_{\Xi}\mathrm{H}) = 2.0$ MeV, is also reported in the work by Friedman and Gal, where an optical potential is employed [31]. But, as discussed in [13], such an agreement could be more or less accidental.

For the ${}^{7}_{\Xi}$H $(\frac{1}{2}^+, \frac{3}{2})$ system, the chiral ΞN potential yields a separation energy of $B_\Xi = 3.50 \pm 0.39$ MeV and a narrow decay width, with $\Gamma = 0.2$ MeV. The computed B_Ξ is only slightly larger than the value of 3.15 MeV reported by Fujioka *et al.* [32] when the HAL QCD potentials is employed in combination with a four-body ($\alpha nn\Xi$) cluster model [33]. With an older $S = -2$ potential from the Nijmegen group, the authors however obtained somewhat smaller binding energy, namely $B_\Xi = 1.8$ MeV [33]. Let us finally remark that in Ref. [13] we have also explored the relation between properties of the employed chiral ΞN interaction and the binding of the A $= 4 - 7$ Ξ systems. We shown that the ΞN attraction in the ${}^{33}S_1$ state is essential for the binding of all the systems considered, which contributes to more than 50% of the ΞN potential expectation value $\langle V_{\Xi\mathrm{N}} \rangle$.

6 Conclusion

In this work, we throughly studied single- and double-strangeness hypernuclei with A $= 4 - 8$ based on the Jacobi NCSM and in combination with the NN (3N), YN and ΞN interactions consistently derived within the chiral EFT approach. In order to speed up the convergence of the NCSM with respect to model space, all the employed two-body and 3N potentials are transformed using an SRG evolution. We explicitly showed that, with the inclusion of the SRG-induced three-body forces (3N and YNN), the strong dependence of B_Λ on SRG flow parameter is removed for ${}^{3}_{\Lambda}$H and significantly reduced for the A $= 4, 5$ systems. After that, we studied the predictions of the two practically phase-equivalent NLO13(500) and NLO19(500) YN interactions for the separation energies in the A $= 4 - 7$ hypernuclei. Both potentials underestimate the ground state of ${}^{4}_{\Lambda}\mathrm{H}(0^+)$. The NLO19 potential yields B_Λ for

${}^{4}_{\Lambda}$H(1^+) and the ground states in ${}^{5}_{\Lambda}$He and ${}^{7}_{\Lambda}$Li that are comparable with the experiments (only slightly above), whereas NLO13 substantially underestimates these systems. We also investigated CSB splittings in the A = 7, 8 multiplets using the two NLO YN potentials that also include the leading CSB interaction in the ΛN channel derived in Ref. [16]. Overall, the predicted CSB for the A = 7 systems are small and agree with experiment while the results for the $A = 8$ doublet are somewhat larger than the available empirical value deduced based on emulsion data. Finally, we discussed our recents results for Ξ hypernuclei with A = 4 – 7 based on the NLO(500) ΞN potential. We found three loosely bound states ($1^+, 0$), ($0^+, 1$) and ($1^+, 1$) for the NNNΞ system. The ${}^{5}_{\Xi}$H and ${}^{7}_{\Xi}$H ($\frac{1}{2}^+, \frac{3}{2}$) hypernuclei are more tightly bound. The decay widths of these Ξ bound states are expected to be very small which could allow them to be observed in experiment.

Acknowledgements: I am very grateful to Ulf-G. Meißner, Johann Haidenbauer and Andreas Nogga for the fruitful collaboration, for proofreading and providing valuable suggestions to improve the manuscript. Numerical calculations have been performed on JURECA and JURECA booster of the JSC, Jülich, Germany.

References

[1] Th. A. Rijken, V. G. J. Stoks, and Y. Yamamoto, Phys. Rev. C **59**, 21 (1999)
[2] J. Haidenbauer *et al.* , Nucl. Phys. A **915**, 24 (2013)
[3] J. Haidenbauer, U.-G. Meißner, and A. Nogga, Eur. Phys. J. A **56**, 91 (2020)
[4] J. Haidenbauer, U.-G. Meißner , and S. Petschauer, Nucl. Phys. **A954**, 273 (2015)
[5] J. Haidenbauer and U.-G. Meißner, Eur. Phys. J. A **55**, 23 (2019)
[6] J. Haidenbauer, Contribution to these proceedings
[7] O. Hashimoto, H. Tamura, Prog. Part. Nucl. Phys. **57** (2005,2006)
[8] S. Liebig, U.-G. Meißner, and A. Nogga, Eur. Phys. J. A **52**, 103 (2016)
[9] H. Le J. Haidenbauer, U.-G. Meißner, and A. Nogga, Eur. Phys. J. A **56**, 301 (2020)
[10] P. Reinert, H. Krebs, and E. Epelbaum, Eur. Phys. J. A **54**, 86 (2018)
[11] P. Maris *et al.* , Phys. Rev. C **103**, 054001 (2021)
[12] E. Epelbaum, Contribution to these proceedings
[13] H. Le, J. Haidenbauer, U.-G. Meißner, and A. Nogga, Eur. Phys. J. A **57**, 339 (2021)
[14] H. Le, J. Haidenbauer, U.-G. Meißner, and A. Nogga, Phys. Lett. B **801**, 135189 (2020)
[15] H. Le, J. Haidenbauer, U.-G. Meißner, and A. Nogga, Eur. Phys. J. A **57**, 217 (2021)
[16] J. Haidenbauer and U.-G. Meißner, and A. Nogga, Few Body Syst. **62(4)**:105, 2021
[17] E. Botta, AIP Conf. Proc., **2130(1)** 030003, (2019)
[18] S. K. Bogner, R. J. Furnstahl, and R. J. Perry, Phys. Rev. C **75**, 061001 (2007)
[19] K. Hebeler Phys. Rev. C **85**, 061001 (2012)
[20] S. Petschauer, N. Kaiser, J. Haidenbauer, and U.-G. Meißner, Phys. Rev. C (2016)
[21] M. Juric *et al*. Nucl. Phys. B **52**, 1 -30 (1973)
[22] M. Agnello *et al*. Phys. Lett. B **698**, 219-225 (2012)
[23] H. Le, J. Haidenbauer, U.-G. Meißner, and A. Nogga (in preparation)
[24] A. Gal, Phys. Lett. B **744** 352 (2015)
[25] E. Hiyama *et al.* , Phys. Rev. C **80** 054321 (2009)
[26] E. Botta, T. Bressani, and A. Feliciello, Nucl. Phys. A **960**, 165 (2010)
[27] R. B. Wiringa, V. G. J. Stoks, and R. Schiavilla, Phys. Rev. C **51** 38 (1995)
[28] E. Hiyama *et al.* , Phys. Rev. Lett. **124** 092501 (2020)
[29] M. M. Nagels and Th. A. Rijken and Y. Yamamoto, arXiv: 1504.02634 (2015)
[30] K. S. Myint and Y. Akaishi, Prog. Theor. Phys. Suppl. **117** 251 (1994)
[31] E. Friedman and A. Gal, Phys. Let B **820** 136555 (2021)
[32] H. Fujioka *et al.* , Few Body Syst. **62** 47 (2021)
[33] E. Hiyama *et al*. Phys. Rev. C **78** 054316 (2008)